MSc in Photonics

Universitat Politècnica de Catalunya (UPC)
Universitat Autònoma de Barcelona (UAB)
Universitat de Barcelona (UB)
Institut de Ciències Fotòniques (ICFO)

http://www.photonicsbcn.eu

PHOTONICS**BCN**

Master in Photonics

MASTER THESIS WORK

NARROWBAND FILTERING FOR ATOM-RESONANT PHOTON PAIR GENERATION

Marc Torrent Cuairan

Supervised by Prof. Dr. Morgan W. Mitchell, (ICFO)

Presented on date 27^{th} October 2017

Registered at

Escola Tècnica Superior d'Enginyeria de Telecomunicació de Barcelona

Narrowband filtering for atom-resonant photon pair generation.

Marc Torrent Cuairan

ICFO, Institut de Ciències Fotòniques, Mediterranean Technology Park, 08860 Castelldefels (Barcelona), Spain

E-mail: marc.torrent@icfo.eu

27th October 2017

Abstract. In this master's thesis we study two filtering techniques, first the Faraday anomalous dispersion optical filter (FADOF) and second a monolithic Fabry-Pérot interferometer with the aim of filtering down-converted photon pairs resonant with the D1 line of ^{87}Rb. The geometrical properties of a plano-convex lens with a high-reflectivity dielectric coating applied on both sides provides us with a long term stability and a tunable Fabry-Pérot cavity suitable for narrowband frequency filtering. A transmission of $\sim$30% is reached, a free spectral range of 19.2 GHz and a bandwidth of 47.5 MHz are measured providing a proof-of-concept for a future implementation. In addition, a 852 nm DFB laser is mounted and tested by performing saturated absorption spectroscopy with the aim of locking the laser. However, the results show that the laser was mode hopping.

1. Introduction

Atom-photon interaction is a key element in quantum information science, understanding its dynamics and being able to describe and control its quantum behavior will allow us to make great steps towards the development of quantum technologies.

Most research in quantum science and technology such as quantum networks [1], quantum memories and repeaters [2], quantum information processing and computing [3], require the generation of photons and its interaction with atoms. For an efficient coupling between the photons and atoms, the linewidth of the photons must be comparable to the atomic transition linewidth, therefore, it is essential to have narrowband photon sources.

Our group is currently working on building a single atom trap experiment. Within a magneto optical trap a ^{87}Rb atom will be confined in a strong optical dipole trap which will allow us to study fundamental aspects of light-matter interaction such as stimulated emission and photon-photon nonlinearities induced by the atom.

A common way to generate atom resonant photonic states for quantum optics experiments is by spontaneous parametric down conversion (SPDC). SPDC sources produce broadband photons which need to be filtered to reduce their bandwidth so they are capable of interacting with atoms. However, by placing the source inside a cavity the bandwidth of the photons is reduced spatially and temporally to the modes permitted in the cavity. But, there are several cavity modes permitted within the phase-matching bandwidth, therefore, there is still a need for spectral filtering to obtain a single mode output. Here, we present a work towards filtering atom resonant photon pairs from a cavity enhanced spontaneous parametric down conversion (CESPDC) so that the frequency of the output photons can be selected.

The master thesis is organized as follows: First, in section 2, I will explain the requirements of our experiment with regards to the photon source and how that affects the type of filtering technique involved. Following this, in sections 3 and 4, I explain the different results obtained when surveying the capabilities of the different filtering techniques. In section 5, the mounting of a 852 nm DFB laser and a saturated absorption spectroscopy of Cs D_2 line is performed.

2. On filtering Photon pairs

For our experiment we alter a previously developed CESPDC source [4] towards obtaining photons in a single mode at the output. Here, we present a work towards filtering photon pairs from a cavity enhanced spontaneous parametric down conversion (CESPDC) so that the output photons can be selected. The source uses a Periodically-Poled KTP (PPKTP) crystal as a nonlinear medium producing photon pairs at the ^{87}Rb D1 transition through type II phase matching. The type II phase matching produces orthogonally polarized signal and idler photons which experience a different temporal walk-off due to the birefringence of the crystal. However, adding an additional KTP crystal increases the difference in FSRs between the signal and idler modes and allows us to control which signal and idler modes are simultaneously resonant. Through this we can achieve simultaneous resonance only in some regions of the spectra, called clusters [4], while satisfying the energy conservation. The clustering effect [5] modifies the SPDC spectra creating 3 clusters separated 68 GHz with 4-5 modes per cluster.

Since the output of the source is still not single mode, spectral filtering is needed. In order to operate at the single mode we need to suppress unwanted modes, which require a filtering system with a bandwidth of less than 490 MHz centered at the frequency of the degenerate mode and resonant to the atomic transition. Additionally, the filter must be tunable to other transitions.

3. Faraday anomalous dispersion optical filter

The FADOF is composed of an atomic vapor cell placed between two crossed polarizers, and a homogeneous magnetic field along the propagation direction of the light [6]. The filtering process occurs due to the resonant Faraday effect where the vapor cell acts as a birefringent medium. The effect leads to a difference in the refractive index of the left and right circular components of the input linearly polarized light induced by the presence of the magnetic field. At the end, it is translated into a polarization rotation of the incident light only for photons which are near an atomic transition, while the others are not rotated. The unrotated photons are blocked by the presence of the second polarizer or absorbed by the medium.

3.1. Theory

A detailed description of the theoretical procedures used for spectra calculation, simulations and the writing of this section can be found in [7].

The Rb hyperfine transitions are described by the Hamiltonian $\hat{\mathcal{H}} = E_F + \hat{\mathcal{H}}_{Ze} + \hat{\mathcal{H}}_{HF}$, where E_F is the energy level including the fine structure contribution and $\hat{\mathcal{H}}_{Ze}$ and $\hat{\mathcal{H}}_{HF}$ are the Zeeman and hyperfine Hamiltonians. The Hamiltonian is diagonalized to find the transition frequencies ($\omega_{ab} \equiv \omega_b - \omega_a$) and their corresponding dipole matrix elements $D_q^{ab} = \langle a| \hat{D}_q |b\rangle$, which describe the strength of the interaction between the ground state and the different excited states, where $q = \pm 1$ describes the polarization of the incident light in the circular basis.

The refractive index that light experiences, $n_q = \sqrt{1 - \chi_{qq}}$, is defined by the electrical susceptibility χ, which is described as

$$\chi_{qq}(\omega) = \sum_{Z\in\{85,87\}} \frac{N_Z(T)}{\varepsilon_0 \hbar} \sum_{a,b} |D_q^{ab}|(\rho_{bb} - \rho_{aa}) V(\sigma, \frac{\Gamma}{2}, \omega_{ba} - \omega) \tag{1}$$

where $N_Z(T)$ is the atomic number density for the isotope Z at temperature T, ε_0 is electrical permitivity, ρ is the atomic density matrix, $V(\sigma, \frac{\Gamma}{2}, \omega_{ba} - \omega)$ is the Voigt profile [8] with $\sigma = \omega_{ab}\sqrt{k_B T/(M_Z c^2)}$. The atomic masses of the isotopes, M_Z,and linewidths, Γ, are taken from [9, 10]. The atom number density is defined as $N_Z(T) = c_Z N_Z^{pure}(T) = c_Z P_Z(T)/(RT)$, where c_z is the isotope abundance, R is the ideal-gas constant and $P_Z(T)$ are the isotope vapor pressures taken from Steck [9, 10].

The transmission of the FADOF is described as $T = |E_{det}^{\dagger} \cdot M_{cell} \cdot E_{in}|^2$ where E_{in} and E_{out} are the Jones vectors for the input and output polarizations, and $M_{cell} = diag(\exp[in_L kL], \exp[in_R kL])$ where k is the wavenumber. The angle of polarization rotation of the filter is

$$\phi = \frac{Re(n_R) - Re(n_L)}{2} kL \tag{2}$$

The magnitude of the polarization rotation is determined by the density of the vapor, the length of the cell, the magnetic field and isotope abundance. By adjusting these parameters we can operate the filter as a narrow-bandwidth optical filter.

3.2. Simulation Results

The existing set-up leads to a peak transmission of 70% at +2.8 GHz from the D_1 center with a FWHM of 445 MHz and 57 dB out-of-band rejection. It has also demonstrated high performance in filtering degenerate photon pairs from a CESPDC source [11]. Our goal is to find the optimum parameters so the filter can be used to fulfill our experimental requirements.

The model I used to compute the spectra of the FADOF at the Rb D1 line was developed by J. A. Zielińska and the Mathematica code to perform the simulations is available in arXiv [7]. ElecSus, a computer program [12] to calculate the electric susceptibility of an atomic ensemble and the spectra of several optical devices including a FADOF, allowed me to perform first level analysis of different configurations which were later analyzed in detail with the Mathematica code.

Table 1 shows a list of possible configurations which could provide filtering according to the requirements described previously.

B (mT)	I(A)	T (°C)	L_{cell} (cm)	^{85}Rb (%)	Transmission (%)	$\Delta\nu$ (MHz)
106.5	69.70	72	19	99.99	96.68	433.95
15.0	9.67	106.5	20	99.99	84.47	582.74
20	12.90	103.5	30	99.99	81.57	337.93
11.2	7.22	123.5	10	99.99	79.48	585.08
12.5	8.06	117.0	20	99.99	71.05	342.08
9.1	5.87	125.5	18	99.99	61.90	346.88

Table 1: Simulation results for different parameter configurations, the suppression of unwanted modes is not shown in the table. The intensities are calculated from [7] and the transmission is measured at the $F = 1 \rightarrow F' = 2$ transition of ^{87}Rb. The highlighted row shows the parameters used in Fig. 1a and 1b respectively. B and I relation is taken from [7] measurements.

Theoretically, it is possible to set-up a FADOF at the $F = 1 \rightarrow F' = 2$ transition of ^{87}Rb with high transmission $\sim 80\%$ and with a good extinction of unwanted modes (Fig. 1a) with roughly 20% transmission of one neighbor mode. However, the different configurations presented and studied are not feasible to be implemented experimentally.

One of the major drawbacks was the requirement for a cell with isotopically pure ^{85}Rb, which is a percentage that vapor cell manufacturers cannot ensure. The cell must be comprised of a species with transitions close to the ^{87}Rb D1 transition for a maximum rotation, but must not contain the ^{87}Rb isotope itself as it would lead to losses due to absorption and we need the photons resonant to the D1 transition in ^{87}Rb to be transmitted out of the filter. Huge magnetic fields ~ 106 mT have to be applied to modify the hyperfine structure such that the desired frequency is not absorbed but transmitted. Therefore, it would need large amounts of current ~ 70 A . Due to the impossibility of implementing the FADOF I had to alter my approach and look for alternative solutions to the filtering.

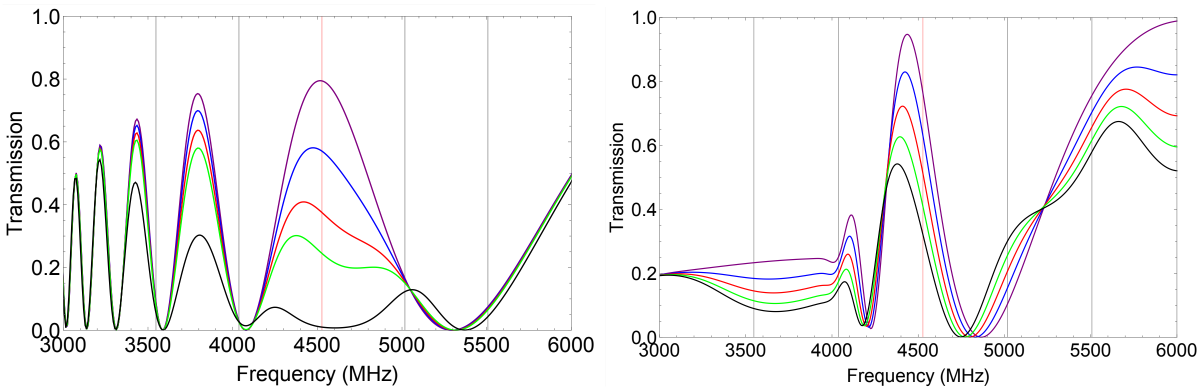

(a) (b)

Figure 1: FADOF spectra calculations (a) for L_{cell} = 100 mm, B = 11.2 mT, T = 123.5°C and different isotope compositions of the vapor alkaline cell: Purple: 99.99% ^{85}Rb, Blue: 99.95% ^{85}Rb, Red: 99.90% ^{85}Rb, Green: 99.85% ^{85}Rb, Black: 99.50% ^{85}Rb. (b) for L_{cell} = 190 mm, B = 106.5 mT, T = 72° C and different isotope compositions of the vapor alkaline cell: Purple: 99.99% ^{85}Rb, Blue: 99% ^{85}Rb, Red: 98% ^{85}Rb, Green: 97% ^{85}Rb, Black: 96% ^{85}Rb.

4. Fabry-Pérot cavities

4.1. Theory

A basic Fabry-Pérot cavity consists of two mirrors, with coefficients for the reflected and transmitted intensity light R_i and T_i respectively, separated by a given distance L. When the frequency resonance conditions are satisfied there is constructive interference of fields within the cavity and light is transmitted, otherwise the cavity blocks the light.

The cavity parameters we are taking into account are:

(i) The free spectral range FSR, which defines the periodicity of the spectrum.

$$FSR = \frac{c}{2nL} \tag{3}$$

where n is the refractive index of the medium and c is the speed of light.

(ii) The cavity Finesse $\mathcal{F}$ can be approximated as

$$\mathcal{F} = \frac{\pi \sqrt[4]{R_1 R_2 (1 - P_{Loss})^2}}{1 - \sqrt{R_1 R_2 (1 - P_{Loss})^2}} \tag{4}$$

where P_{Loss} are the intracavity losses, see [13].

(iii) The cavity bandwidth $\Delta\nu$ or FWHM is defined as the distance in frequency between the half-maximum points.

$$\Delta\nu = \frac{FSR}{\mathcal{F}} \tag{5}$$

Experimentally we need to take into account several things that will affect the transmission properties of the FP. The most important factors contributing to a low transmission are the absorption losses in the medium and the scattering losses from each mirror surface. Further losses occur if the incident light is not perfectly aligned to the cavity mode.

4.2. Monolithic Fabry-Pérot filter cavity

Our cavity consists of a standard commercial plano-convex lens coated on both sides with a high reflectivity dielectric coating and allow us to combine the stability of a monolithic etalon with the spatial mode filtering allowed by FP cavities [14, 15]. Changing the temperature T of the cavity changes its length L and its refractive index n allowing us to be able to tune the cavity to a particular resonance.

The design parameters such as length, radius of curvature and reflectivity can be calculated from the desired final specifications. For our experiment, a transmission of $\sim 80\%$, and extinction ratio of ~ 50dB and a bandwidth smaller than the free spectral range of the CESPDC < 490 MHz should satisfy experimental needs.

4.3. Design and characterization

To obtain the desired results a lens, see Table 2, is purchased:

Type	Material	Diameter	Thickness	Radius	Focal length	Reflectivity @795 nm
PCX	BK7	25.4 mm	5.3 mm	40.68 mm	80 mm	99% +/-0.5%

Table 2: Specifications of the lens provided by Lambda Research Optics inc.

Two conditions must be satisfied for transmission of light through the cavity:

(i) Standing wave condition: The laser frequency should match the cavity resonance frequency.

(ii) Stable mode condition: The laser beam waveform must match the curvature of the cavity output mirror and when it is reflected back to the input mirror it must have the same waist size.

The first condition is satisfied via temperature tuning the lens. A special lens holder (Fig. 2) is designed to ensure the stability required, a bad control of the temperature can affect the filtering performance causing fluctuations on the output power.

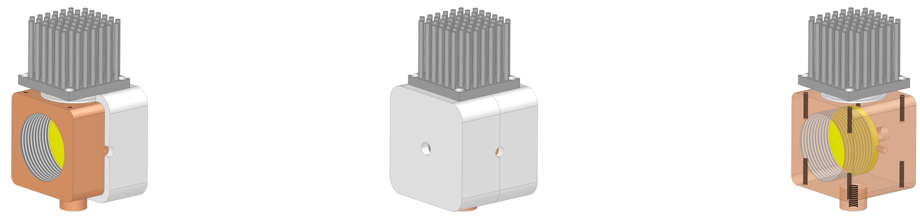

Figure 2: Mechanical design of the lens holder. A copper cube with 1-inch hole for the lens. The plano side of the lens is mounted on top of a silicone thermal interface in contact with the copper and retained with a standard retainer ring. A teflon shell with a 5mm hole acts as an insulator. A peltier is placed on top in contact with an aluminum heat sink. For temperature stabilization a 10 kΩ NTC sensor is placed under the peltier.

The second condition is fulfilled when the wave front of the incident beam matches the waist and curvature of the cavity. The waist of our cavity is calculated to be $w_0 = 47.89\ \mu$m and the radius of curvature of the wavefront must match the radius of the convex curvature $R = 40.68$mm. The experimental set up for accomplishing the mode matching conditions is shown in Fig. 3.

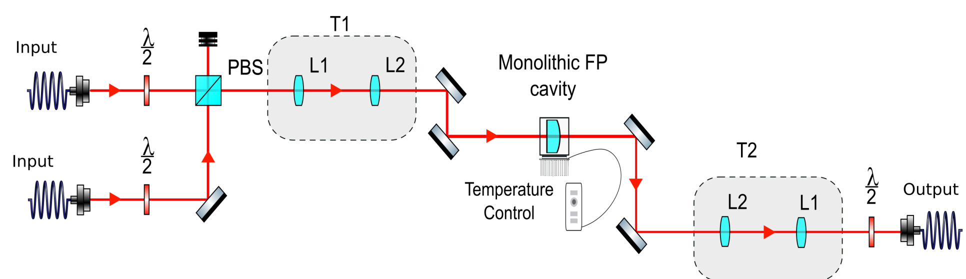

Figure 3: Experimental set up for filtering polarization atom resonant photon pairs.

The photons enter the filtering process from the input fiber couplers, afterwards, its polarizations is adjusted with a $\lambda/2$ wave plate. Then, the two beams are merged in a polarization beamsplitter (PBS). The telescope T1 consists of two lens L1 and L2 with 60mm and 40mm of focal length respectively to modify the wave front to match the cavity mode. After the telescope, two mirrors adjust the alignment of the beam to the cavity. The cavity is mounted into the holder and positioned on a translational stage with the light focusing on the plano side. A second telescope T2 is used to collimate the beam and finally, the light is coupled to fiber. Both telescopes are mounted in a cage system and L1 is mounted on a micrometrical stage for fine tuning. The set up is divided in two equal parts in case different frequencies need to be filtered, only one part is shown in Fig. 3.

4.4. Simulations and experimental results.

The simulations for the cavity characteristic parameters give us a FSR= 18.72 GHz, a finesse of $\mathcal{F} = 488$ and a bandwidth of $\Delta\nu = 38.37$ MHz.

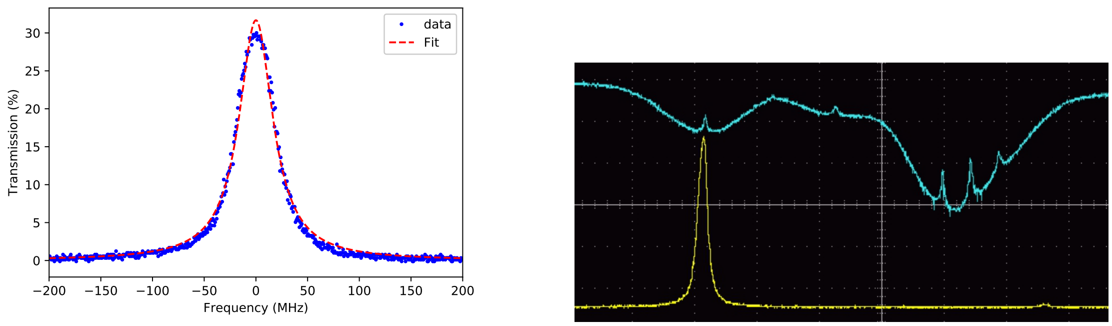

Figure 4: Left: Experimental cavity transmission mode with a Lorentzian fit. Right: The yellow line shows the cavity spectrum compared to the blue SAS signal of Rb.

To measure the FSR I measured the current difference between two gaussian modes. I converted the change in current of the laser to change in frequency using an atomic transition as reference. The experimental FSR is measured to be 19.2 GHz. The bandwidth of the cavity was measured by fitting a Lorentzian to a cavity transmitted mode data taken by an oscilloscope (Fig. 4 Left). The value measured is $\Delta\nu = 47.5$ MHz. Finally, a experimental finesse of $\mathcal{F} = 404$ is calculated. The maximum measured transmission of the resonant frequency is $T_{max} \sim 30\%$. With this calculation we can estimate the losses we have inside the cavity. By comparing the measured value with (4) we can conclude that we are having between 0.1%-0.2% of P_{Loss}.

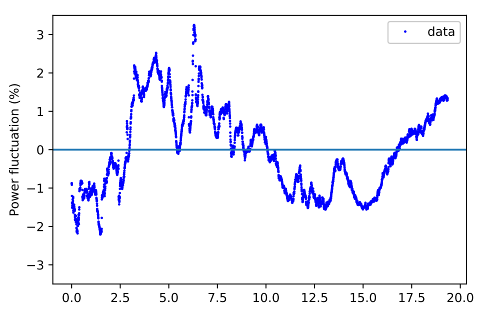

Figure 5: Power fluctuations of the cavity resonant output light. After 20min a maximum of 3% fluctuation is measured.

To measure the temperature stability I monitored the resonant cavity peak output power to measure its fluctuations. Since the measurements are taken after a PBS, the light polarization changes translate into changes in power. In order to be able to separate the two fluctuations, I have measured the fluctuations on the other side of the PBS where only the polarization fluctuations will appear. Then, I removed the polarization fluctuations to the measurements after the cavity. A maximum of 3% of fluctuation was measured (Fig. 5).

5. Saturated absorption spectroscopy of Cs

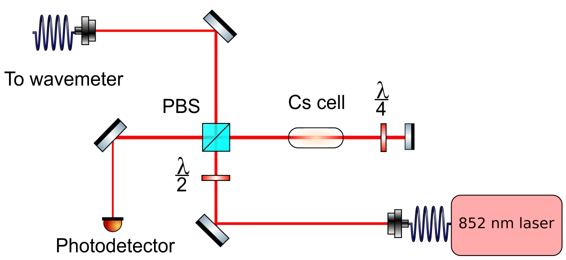

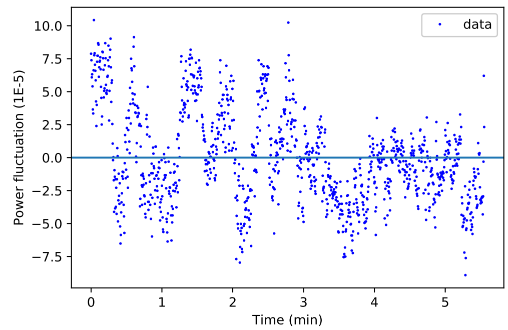

Figure 6: Left: Experimental setup for doing saturated absorption spectroscopy of Cs Part of the light is sent to a wave meter to know the wavelength. PBS: polarization beamsplitter. $\frac{\lambda}{2}, \frac{\lambda}{4}$: half and quarter wave plates. Right: Measured power fluctuations at the fiber output of the 852nm laser.

A 852 nm DFB laser will be used for creating the dipole trap for the single atom. Though the dipole trap itself does not need the light to be frequency locked, to create lattices we require stable standing waves and it will might be of our interest to lock the laser. Also, by having the dipole light locked this can be easily filtered out by means of absorption in a Cs vapor cell. The setup is shown in Fig. 6. I mounted the laser and performed a saturated absorption spectroscopy (SAS), however, the results show that the laser was mode hopping and it not possible to lock it by SAS. To measure the power stability of the laser In a second experiment I monitored the laser power at the output of the laser fiber with a power meter at a fixed laser current and temperature. The results (Fig 6 Right) showed small power fluctuations.

6. Conclusions

I have shown that implementing a FADOF for filtering photon pairs at the $F = 1 \rightarrow F' = 2$ transition of ^{87}Rb was not experimentally feasible. The system is not capable of fulfilling our requirements. Then I have studied and analyzed a new type of FP cavity as a proof-of-concept, the monolithic FP cavity is able to achieve frequency and spatial filtering in combination with an easy tunability to other transitions by just adjusting the temperature of the cavity. We have designed a temperature controlling and holding system that was tested showing a maximum of ∼3% fluctuation in 20min. The cavity has been experimentally characterized to have a FSR of 19.2 GHz, a bandwidth of $\Delta\nu = 47.5$ MHz and a maximum transmission of ∼30%. The high reflectivity coatings combined with the intracavity loss are the causes of having low transmission. High reflectivity means high finesse and narrower bandwidth, but it is sufficient for us to have a bandwidth smaller than output FSR of the CESPDC, 490 MHz. Therefore, the reflectivity of the coating can be reduced and, consequently, the bandwidth and transmission will increase. A R=95-96% will produce a bandwidth between $200 - 300$ MHz and the transmission will increase because the photons will escape the cavity before they are lost. Super-polishing the mirror surfaces will reduce scattering losses from the surfaces. These changes would make the mode matching less tedious and improve the results significantly.

Acknowledgements

I am deeply grateful to Vindhiya for her guidance and patience during these months; to Natalia, Lorena and Alvaro for their guidance inside the lab, and specially to Morgan, for giving me this amazing and unique opportunity to work with him. I would also like to thank my family and especially to Carla for supporting me all this time.

References

[1] H. J. Kimble, *The quantum internet.* Nature 453, 1023-1030 (2008).

[2] Simon C, De Riedmatten H, Afzelius M, Sangouard N, Zbinden H and Gisin N. *Quantum Repeaters with Photon Pair Sources and Multimode Memories.* Physical Review Letters 98, 190503 (2007)

[3] L. Duan, M. Lukin, J. Cirac and P. Zoller. *Long distance quantum communication with atomic ensembles and linear optics.*

[4] F Wolfgramm, X Xing, A Cerè, A Predojević, A M Steinberg, and M W Mitchell. *Bright filter-free source of indistinguishable photon pairs.* Opt. Express, 16(22): 18145-18151, Oct 2008.

[5] E. Pomarico, B. Sanguinetti, C. I. Osorio, H. Herrmann, and R. T. Thew. *Engineering integrated pure narrow-band photon sources.* New Journal of Physics, 14(3): 033008, 2012.

[6] D. J. Dick, T. M. Shay, *Ultrahigh-noise rejection optical fillter*, Opt. Lett., vol. 16, p. 867, (1991).

[7] J. A. Zielińska, F. A. Beduini, N. Godbout and M. W. Mitchell. *Ultranarrow Faraday rotation filter at the Rb D_1 line.* Opt. Lett. 37, 524 (2012). arXiv:1110.2362

[8] G. Pagnini and R.K. Saxena. *A note on the Voigt profile function.* arXiv:0805.2274

[9] Daniel A. Steck, *Rubidium 85 D Line Data* (revision 2.1.6, 20 September 2013)

[10] Daniel A. Steck, *Rubidium 87 D Line Data* (revision 2.1.5, 13 January 2015)

[11] J. A. Zielińska, F. A. Beduini, *Atomic filtering for hybrid continuous-variable/discrete-variable quantum optics.* Opt. Express 22, 25307-25317 (2014).

[12] Zentile, M. A. et al. *ElecSus: A program to calculate the electric susceptibility of an atomic ensemble.* Comput. Phys. Commun. 189, 162-174 (2015).

[13] F. Wolfram. *Atomic quantum metrology with narrowband entangled and squeezed states of light.*. PhD Thesis. Barcelona, December 2011.

[14] P. Palittapongarnpim, A. Macrae and A. I. Lvovsky. *A Monolithic Filter Cavity for Experiments in Quantum Optics.* Review of Scientific Instruments 83, 066101 (2012) .

[15] A. Ahlrichs, C. Berkemeier, B. Sprenger and O. Benson. *A monolithic polarization-independent frequency-filter system for filtering of photon pairs.* Appl. Phys. Lett. 103, 241110 (2013).